

Article

Modification of Recovered Silicon from End-of-Life Photovoltaic Panels for Catalytic Reduction of Cr(VI)

Charalampos Pavlopoulos ¹, Konstantina Papadopoulou ^{1,*}, Minas Theocharis ², Petros Tsakiridis ², Pavlina Kousi ², Artin Hatzikioseyan ², Emmanouella Remoundaki ² and Gerasimos Lyberatos ^{1,3}

¹ School of Chemical Engineering, National Technical University of Athens, Iroon Polytechniou 9, Zografou, 15780 Athens, Greece

² School of Mining and Metallurgical Engineering, National Technical University of Athens, Iroon Polytechniou 9, Zografou, 15780 Athens, Greece

³ Institute of Chemical Engineering Sciences (ICE-HT), Stadiou Str., Platani, 26504 Patras, Greece

* Correspondence: kpapado@chemeng.ntua.gr; Tel.: +30-217723115

Abstract: As installed photovoltaic panels (PVPs) approach their End of Life (EoL), the need for a sustainable recovery plan becomes imperative. This work aims to reuse silicon from EoL PVPs as a potential catalyst/photocatalyst for wastewater treatment. PVPs were pretreated thermally. The resulting mixture was separated into different fractions using a trommel screen. Recovered silicon flakes were cleaned with HNO₃ and HF in order to obtain pure Si, which was then etched through a single stage Ag-assisted Chemical Etching process and decorated with Ag/Cu. Photocatalytic reduction of Cr(VI) in the presence of 5 mM citric acid was carried out in a 600 mL batch reactor irradiated by a Xenon 150 W arc lamp as well as under dark conditions. It was found that, in the presence of 1.2 g/L of Si catalyst, Cr(VI) at an initial concentration of 15 mg/L can be reduced below the detection limit (>99%), even under dark conditions, in 30–180 min, depending on the pH of the solution and the citric acid concentration. Citric acid was proved to assist the reaction in three ways: lowering the pH, increasing the solubility of the precipitate, preventing inhibition, and as sacrificial agent in photocatalysis. Irradiation, however, was shown to possibly inhibit the process if the citric acid concentration is low.

Keywords: hexavalent chromium reduction; photocatalyst; photovoltaic panel; silicon recovery; wastewater treatment



Citation: Pavlopoulos, C.; Papadopoulou, K.; Theocharis, M.; Tsakiridis, P.; Kousi, P.; Hatzikioseyan, A.; Remoundaki, E.; Lyberatos, G. Modification of Recovered Silicon from End-of-Life Photovoltaic Panels for Catalytic Reduction of Cr(VI). *Waste* **2023**, *1*, 81–94. <https://doi.org/10.3390/waste1010006>

Academic Editor: Giovanni De Feo

Received: 10 October 2022

Revised: 19 November 2022

Accepted: 22 November 2022

Published: 25 November 2022



Copyright: © 2022 by the authors. Licensee MDPI, Basel, Switzerland. This article is an open access article distributed under the terms and conditions of the Creative Commons Attribution (CC BY) license (<https://creativecommons.org/licenses/by/4.0/>).

1. Introduction

Over the past decades, the use of solar Photovoltaic Panels (PVPs) to harness solar energy has been widely expanded. Globally installed solar PVPs capacity exceeded 200 gigawatts (GW) by the end of 2015 and has been estimated to rise to up to 4500 GW by 2050. As installed first and second generation solar PVPs approach the end of their 30-year average lifespan in the early 2030s, recycling, reuse, and safe disposal of solar PVPs waste are becoming a critical and global challenge to prevent thousands of metric tons of this Waste from Electrical and Electronic Equipment (WEEE) to be laid in landfills [1].

As the volume of End-of-Life (EoL) solar PVPs waste is expected to reach millions of metric tons in the upcoming decades, researchers around the world are focusing on the characterization of this upcoming type of waste [2] as well as its possible environmental [3] and economic impacts [4], highlighting the importance of recovering critical materials, like crystalline silicon wafers from first generation PVPs and thin films from second generation PVPs, that contain heavy metals like Cu In (Ga) Se or CdTe. Even in the case of more advanced third generation PVPs that are not widely commercially available, the nanotechnologies used introduce an extra risk of nanoparticles leaching to the environment. In all cases, toxic materials can leach into landfills and subsequently into the environment,

with direct impact on the ecosystem or an indirect impact on humans through the water cycle [5].

The first generation of EoL solar PVPs that use monocrystalline and polycrystalline silicon as semiconductor have already concerned researchers since the beginning of the century in terms of possible material recovery. For the recovery of silicon wafers from a panel, use of chemical methods [6] has lost ground to physical and/or thermal treatment processes [7], as the latter prove to be more environmentally and economically sustainable. In a previous work, an integrated hydrometallurgical process for the recovery of pure crystalline Si and Ag from EoL Si PVPs has been proposed [8]. Advances have also been made in the case of second generation PVPs, as a hydrometallurgical process for the recovery of indium and gallium has been proposed [9].

There is extensive research on material recovery and recycling [4,6,7,10,11]; however, there is a gap concerning the potential reuse pathways of recovered semiconductors from EoL PVPs. The utilization of recovered crystalline silicon is important due to the high temperature requirement for its manufacturing. In previous work, the potential utilization of first and second generation PVP waste as aggregate in Portland cement was examined. Mortar samples containing second generation PVP waste exhibited enhanced mechanical strength and durability, indicating it can be reused as aggregate in construction, simultaneously stabilizing metals like Cu, In, Ga, Se. However, in the case of the mortar samples containing first generation PVP waste, gas formation in the cement paste led to decreased performance [12]. In the current case, a process that takes advantage of the silicon's semiconductor properties was examined.

Silicon's ability to absorb solar light, along with other properties of its nanostructures, renders it a potential catalyst for solar driven applications [13]. A common process employed to form crystalline silicon into a catalyst is metal assisted chemical etching. Through this process a (nano) wire structure is formed on silicon's surface, increasing its specific surface area [14,15]. For photocatalytic applications, as silicon struggles due to its low energy bandgap, pairing it with other catalysts or noble metals is common practice. Specifically, through a simple chemical electroless deposition process, metals like Pt, Au, Ag and Cu have been shown to increase silicon's photocatalytic activity [13,16–18]. Such catalysts, prepared from commercial crystalline silicon, have shown enhanced photocatalytic effectiveness in wastewater treatment applications. The pollutants whose degradation has been investigated mostly include organic dyes [17–19]; hexavalent chromium reduction has also been reported [20]. The latter holds great interest due to the strong oxidizing properties of hexavalent chromium, which render it one of the most carcinogenic and toxic substances produced by natural and anthropogenic processes. It occurs mostly in industrial waste streams, municipal waste landfill, metal mineral extractions and agricultural activities (e.g., pesticides, fertilizers) [21].

A significant rise in waste originating from end-of-life photovoltaic panels is expected in the upcoming decades, as the world is turning towards renewable energy sources. Therefore, a sustainable management plan for recovering and reusing critical materials in photovoltaic panels becomes imperative. Researchers have so far focused mainly on material recovery. This study approached the recyclability issue by focusing on the utilization of crystalline silicon contained in first generation solar cells and the possibility of reusing the material in wastewater treatment applications. A Silicon NanoWire (SiNW) catalyst was prepared from the PV recovered silicon through simple chemical methods that are commonly used on commercial, high-cost crystalline silicon wafers. Sufficient photocatalytic Cr(VI) reduction was achieved both with solar irradiation and even in dark conditions, which was not reported in previous works that use SiNWs for Cr(VI) photoreduction.

The purpose of the present work was to investigate the potential of elaborating Si nanostructures using Si recovered from EoL first generation PVPs as a catalyst in wastewater treatment, in particular for the reduction of hexavalent chromium. Metals already existing in the PVPs (Ag, Cu) in small amounts are retained in the Si structure, in order to develop an economically meaningful utilization procedure.

2. Materials and Methods

2.1. Materials

First generation monocrystalline and polycrystalline Si end-of-life PVPs (manufactured by Hyundai) that were installed in Greece, were provided by POLYECO S.A. after their decommissioning from the field; copper (II) sulfate 5-hydrate (99%), hydrogen fluoride (48%), nitrates of silver (99.8%) and acetone (99.5%) were obtained from Panreac–AppliChem. Nitric acid (65%) was obtained from Honeywell–Fluka. Citric acid monohydrate (99%), hydrochloric acid (37%) and $K_2Cr_2O_7$ crystals were obtained by Sigma-Aldrich.

2.2. Silicon Recovery

First generation crystalline silicon EoL solar PVPs were manually cut into 40×30 mm pieces and placed in a furnace in porcelain crucibles at $550 \text{ }^\circ\text{C}$ for 30 min to remove polymer sheets of ethylene vinyl acetate (EVA). The resulting mixture of Si flakes, soda lime glass, electrodes and ash was separated in a trommel screen. Glass used in PVPs is common hardened soda lime glass with low iron content. Copper electrodes were collected separately due to their high value. The process is displayed schematically in Figure 1.

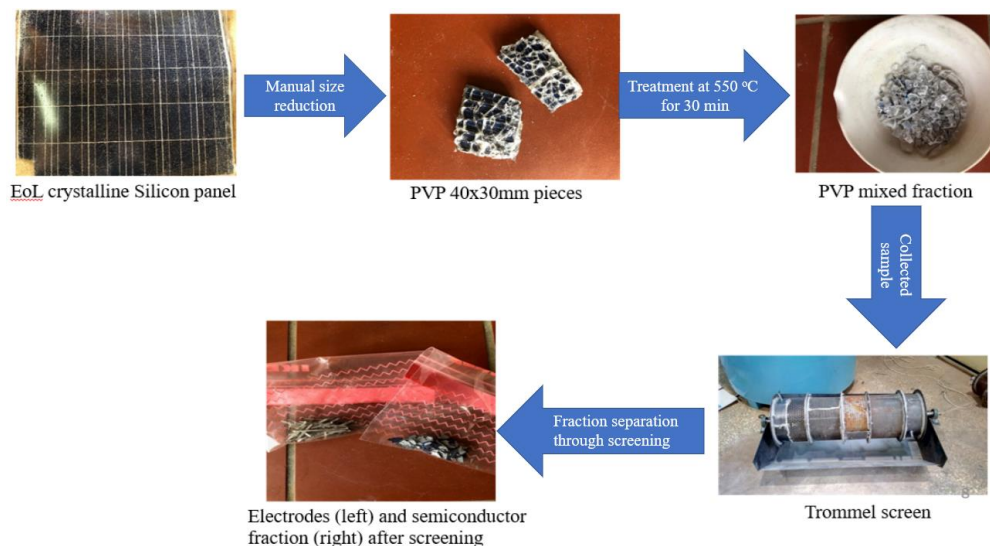


Figure 1. Material recovery process from first generation End-of-Life (EoL) photovoltaic panels (PVPs).

Semiconductor fraction consists mainly of crystalline silicon covered with Anti-Reflective Coating (ARC) (Si_3N_4) on the front side and an aluminum layer on the back side. The fraction containing Si flakes was washed with deionized water and acetone to remove ash and residues, followed by 4N HNO_3 treatment, and then shaken at 200 rpm for 24 h. The samples were also treated with 10% *w/w* HF aquatic solution for 3 h to remove the Anti-Reflective Coating, Al coating and oxides from their surface. Both acid treatments were performed at a ratio of 5 g of Si flakes to 100 mL acid solution. Finally, the flakes were dried and ground.

2.3. Silicon Modifications

The first process was a single step Ag-assisted chemical etching, which aimed to create high surface area Nano Wire structures on Si surface (SiNW). Si powder was immersed for 30 min in a 4.6 M HF aquatic solution containing 0.035 M $AgNO_3$ maintained at $55 \text{ }^\circ\text{C}$ using a water heat bath. Etching was performed using 40 mL of etching solution per gram of silicon. The Ag deposited on the silicon surface was removed using a 10% *w/w* HNO_3 solution for 5 min in samples that were afterwards decorated only with Cu, in a ratio of 40 mL solution per gram of silicon. After etching, Si oxides were removed from the

sample's surface using 10% *w/w* HF aqueous solution for 1 min, in a ratio of 40 mL solution per gram of silicon. Finally, the samples were rinsed with deionized water until reaching a neutral pH and dried at 105 °C for 24 h.

The second process employed was a simple deposition of Cu on the etched Si surface that aimed to create a Schottky barrier that acts as an electron trap. This barrier inhibits the recombination of photo-generated electron/hole pairs, assisting the photocatalytic mechanism. It was carried out for 2 min at room temperature in 1.4 M HF aquatic solution containing 0.035 M $\text{CuSO}_4 \cdot 5\text{H}_2\text{O}$. Doping was performed using 40 mL of etching solution per gram of silicon.

Four different samples were collected using the above modifications. All of them were subjected to chemical etching. One was without metal decoration (SiNW), one was Ag decorated (SiNWAg), one was decorated with Cu (SiNWCu) and one was decorated with both metals (SiNWAg/Cu). Their performance was tested in hexavalent chromium degradation, and the most efficient was used for the rest of the experiments.

2.4. Characterization

The morphology of the samples was examined by Scanning Electron Microscopy (SEM) using a Jeol 6380 L V Scanning Electron Microscope. Experimental conditions involved 20 kV accelerating voltage, using both backscattered and secondary electron detectors. Spot chemical analysis of the sample particles was carried out by an Oxford INCA Energy Dispersive Spectrometer (EDS) connected to the SEM. X-ray Diffraction (XRD) spectra were obtained by a BRUKER D8 ADVANCE diffractometer in a powder sample. Resulting diffraction peaks were identified through the software database.

2.5. Photocatalytic Experiments

A hexavalent chromium solution with an initial concentration of 15 mg/L was prepared by dissolving $\text{K}_2\text{Cr}_2\text{O}_7$ powder in deionized water. The photocatalytic degradation was carried out by dispersing the catalyst's powder into 600 mL of the aqueous solution of $\text{K}_2\text{Cr}_2\text{O}_7$ under stirring at 600 RPM, in the presence of 5 mM of citric acid, which acts as an electron donor. The solution was then irradiated with simulated solar light from a 150 W Xenon arc lamp immersed in the reactor (Figure 2) for 240 min using an immersion tube. The concentration of hexavalent chromium was measured by the 1,5-Diphenylcarbazide photometric method at a 540 nm wavelength using an UV-VIS HACH LANGE DR6000 spectrophotometer, as described in "Standard Methods for Examination of Water & Wastewater". Catalytic experiments were carried out in the same conditions without using the Xenon arc lamp.



Figure 2. Photoreactor set up by Peschl Ultraviolet GmbH—Mainz, Germany; radiation protection cabinet; power supply and cooling unit (**left**); photoreactor vessel (**center**); vessel parts (**right**).

3. Results

3.1. Morphology after Cleaning

In Figure 3, SEM images of recovered silicon flakes before and after the cleaning process are presented. Comparison of Figure 3a,b,e,f indicates that the HF treatment efficiently removed both the ARC from the front side and the Al coating from the back side of the Si flake. In Figure 3c,d, it can be observed that the HNO₃ removed the Ag electrode from the front side, although a few residues still exist. Figure 3b,d show that pores were formed in the front side after the etching of anti-reflective coating, and this might affect the direction of the following Ag-assisted chemical etching process.

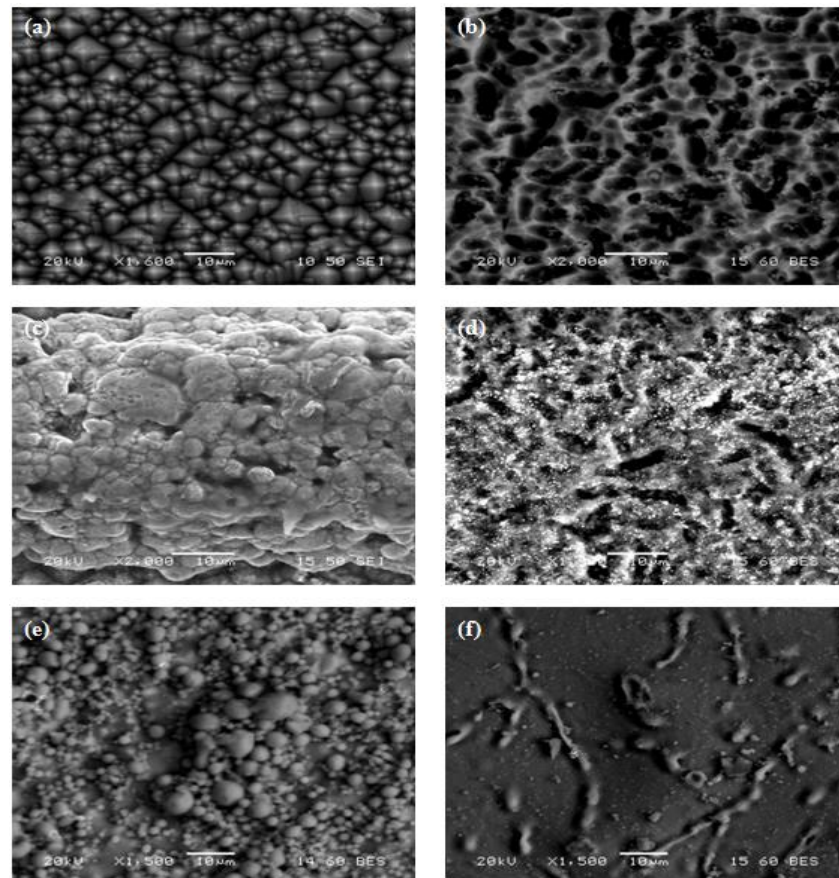


Figure 3. Scanning Electron Microscopy (SEM) images of recovered polycrystalline Si flakes before cleaning (a,c—front, e—back) and after cleaning (b,d—front, f—back).

3.2. Morphology after Modification

SEM images of silicon powder modified using Ag-assisted chemical etching and doping with Ag and Cu are presented in Figure 4. Upon examining Figure 4a, pits and wire bundles can be observed. The observed agglomeration of the wire tips is attributed to Van Der Waal forces [15,17]. The etching has not been homogeneous and vertical due to the various crystallographic orientations of the polycrystalline powder. The etching appears limited because it is oriented preferably in (100) plane, since the Si atoms on the (100) planes have two covalent bonds connected to the substrate, while the (111) and (110) planes are much denser, with more than two bonds [18,22]. Those dense planes are dominant in recovered polycrystalline Si according to the XRD scan of Figure 5a, leading to slow etching rates. An Ag film was partially formed on the etched surface (Figure 4a), and a thin layer of Cu totally covered the etched silicon's surface (Figure 4b). The latter might prohibit irradiation of the photocatalyst's surface, potentially lowering its effectiveness.

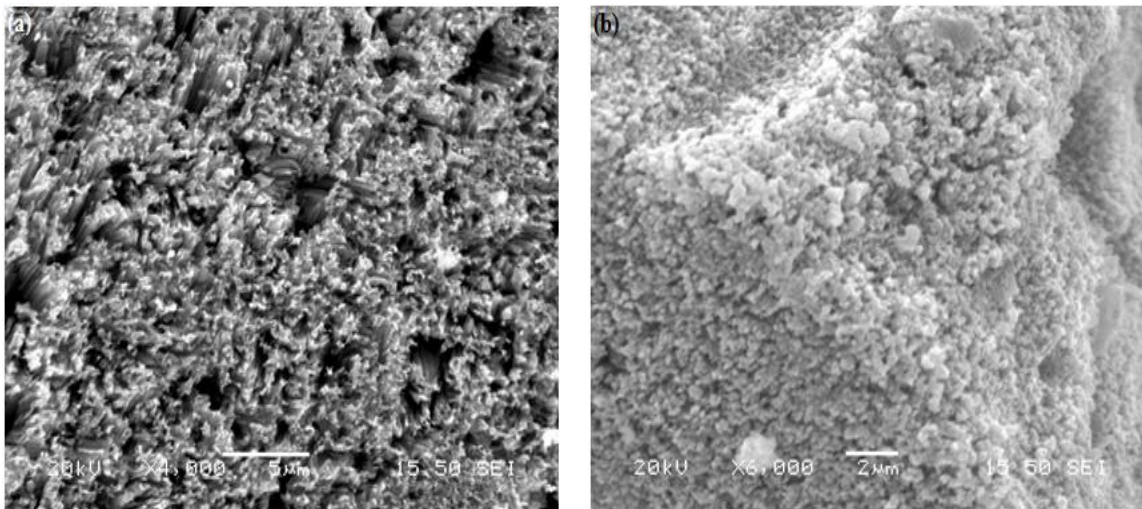


Figure 4. SEM images of recovered EoL PVP polycrystalline Si after etching and decorated with (a) Ag, (b) Cu.

Figure 5 displays XRD scans of the PV Polycrystalline recovered silicon. In Figure 5a, the characteristic peaks of polycrystalline silicon at 28.4° (111), 47.3° (220), 56.1° (311), 69.1° (400), 76.4° (331) and 88° (422) after cleaning indicate, as aforementioned, that (111) and (110) are the dominant crystallographic planes of the sample. Comparing the distribution of planes in Figure 5a–c, there is a notable decrease of the initially dominant planes' ((111) and (110)) intensity after etching and doping. Specifically, in the case of Ag doping, only the (311) plane has a slight increase, whereas, in the case of Cu doping, there is a slight increase in (422). The Cu cations observed in Figure 5 are attributed to copper oxides, possibly created during drying of the sample, since copper can be oxidized by air.

3.3. Hexavalent Chromium Reduction

Three control reduction experiments were carried out in hexavalent chromium solutions of an initial concentration of 15 mg/L without a catalyst, using:

1. Solar irradiation;
2. 5 mM citric acid;
3. A combination of both.

In all three cases, after 240 min of the experiment, the reduction observed was negligible (<2%), meaning that in the absence of a catalyst, the radiation and organic acid have no effect on chromium reduction.

The photocatalytic performance of four different catalysts, prepared as described in Section 2.3, was tested. The ratio of the concentration (C) to the initial concentration (C_0) of hexavalent chromium for 240 min is presented in Figure 6. SiNWs with no metal decoration exhibit a slight decrease in chromium concentration within the first 30 min of the experiment with no further reduction, indicating that there is sorption of the pollutant on the silicon surface but no subsequent photocatalytic activity. Samples decorated with Ag or Cu display similar performance, achieving totals of 50 and 55% reduction, respectively. Most efficient was the sample decorated with both Ag and Cu, as it reduced 80% of the chromium concentration after 240 min, achieving a reaction constant k of 0.0078 min^{-1} with R^2 of 94.01%. Based on these results, the following experiments were carried out with a sample of SiNWAg/Cu.

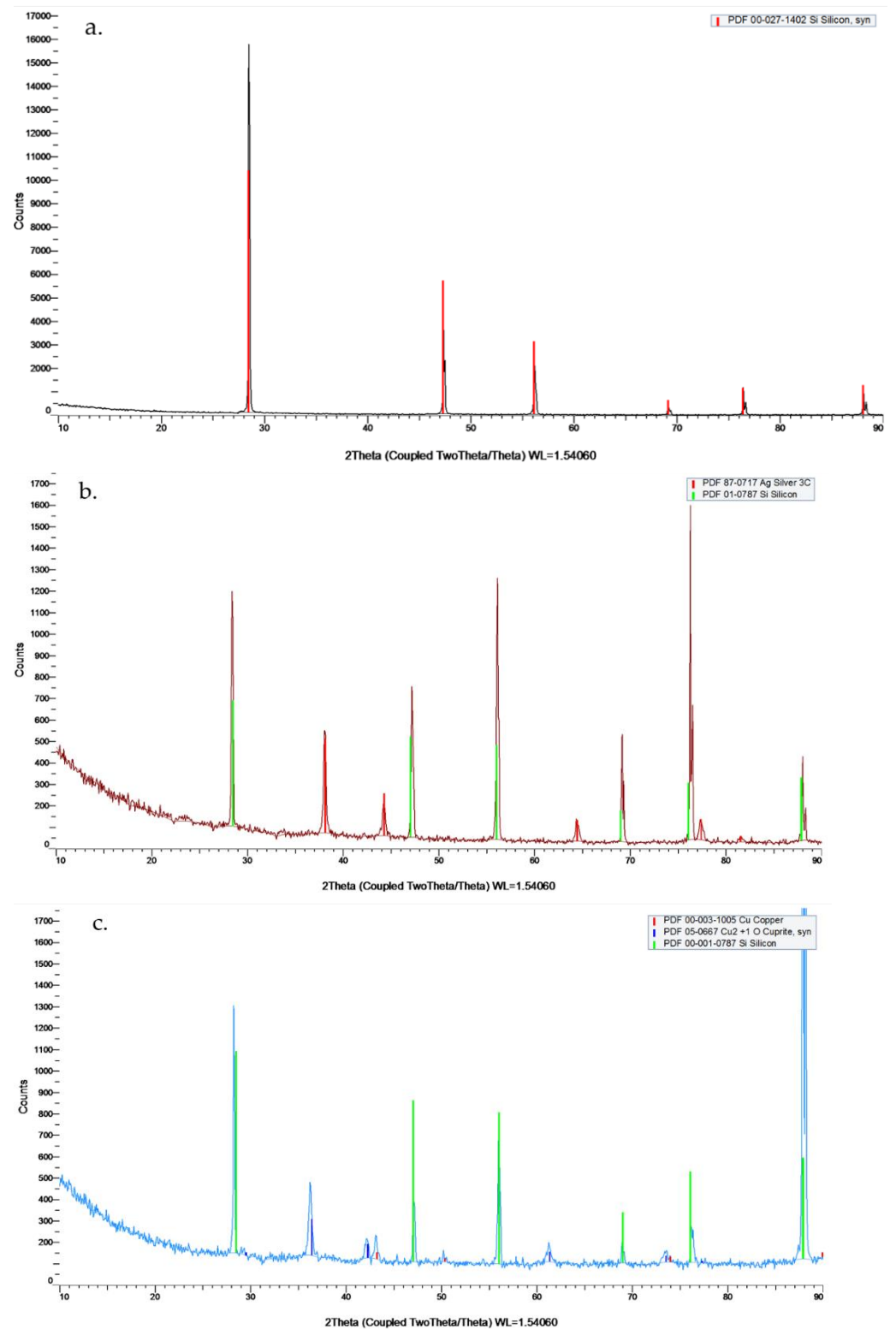


Figure 5. XRD scans of recovered polycrystalline Si (a) after cleaning, after etching and doping with (b) Ag, (c) Cu.

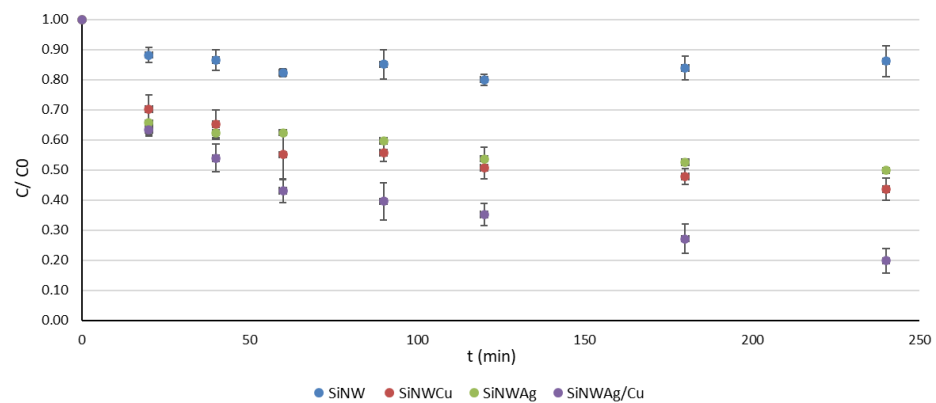


Figure 6. Duplicates of solution of $C_0 = 15$ mg/L Cr(VI), 5 mM citric acid and 1.2 g catalyst/L, under solar irradiation, at pH 2.8.

The effect of the catalyst was also tested in the absence of citric acid, both with and without solar irradiation. In both cases, chromium reduction was also negligible, indicating in turn that the presence of both citric acid and a catalyst is mandatory for the reduction of hexavalent chromium.

Experiments with the simultaneous presence of 1.2 g/L of catalyst and 5 mM of citric acid in the absence of irradiation were carried out to determine the effect of simulated solar irradiation in hexavalent chromium reduction. An increase in reduction rate was expected, according to previous reports [20], in the case of irradiation provided to the system; however, the experimental runs under dark conditions developed better reduction rates. As this phenomenon raised questions regarding the nature of the reaction, the experiments were repeated in triplicates. The average values of the ratio of the concentration (C) to the initial concentration (C_0) and the standard deviation are presented in Figure 7. After 240 min of irradiation, $81 \pm 4\%$ reduction was observed, compared to a total of $91 \pm 3\%$ under dark conditions, proving that the reaction is not photoinduced and that, in current conditions, it was inhibited by providing irradiation, as the observed reaction constant k for dark conditions was 0.0123 min^{-1} with R^2 of 94.50%, 1.58 times higher than the corresponding rate when solar irradiation was provided to the system.

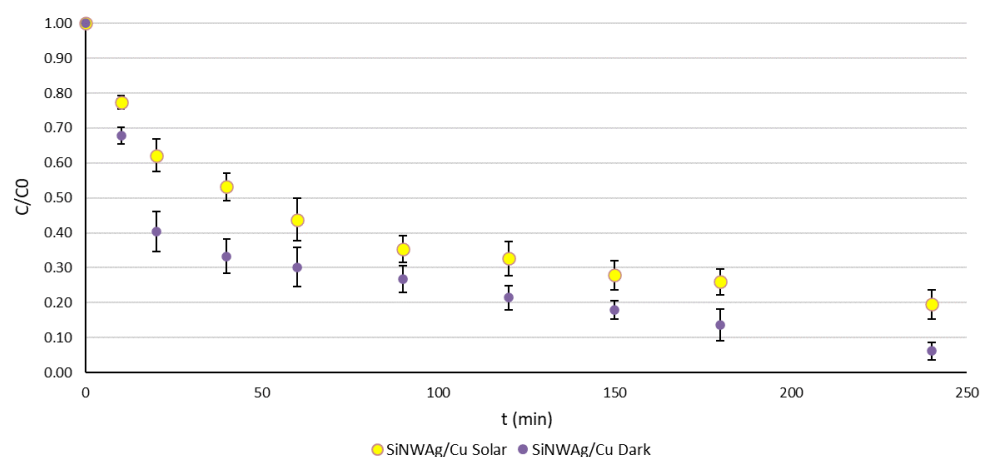


Figure 7. Triplicates of $C_0 = 15$ mg/L Cr(VI) reduction, in the presence of 5 mM citric acid and 1.2 g catalyst/L, under simulated solar irradiation and dark conditions, at pH 2.8.

An occurrence of slight fluctuations of the pH in the DI system at the time of the experiments revealed that the progress of the reaction is sensitive to and dependent on even small pH fluctuations. Three experiments conducted in pH 2.5, 2.7 and 2.9 are presented in Figure 8 in comparison with the behavior in the typical pH of 5 mM of citric acid solution (2.8). It is observed that the performance increases with decreasing pH and complete

reduction is achieved for a pH below 2.7, even in 60 min of reaction for a pH value of 2.5. In higher pH values (2.8, 2.9), reduction seems to be inhibited, probably due to a decrease of Cr(III) solubility. This phenomenon is important, as it highlights the effect of the interaction between chromium reduction products, mainly Cr(III) precipitates that might inhibit the reaction, and the catalyst surface. The maximum reaction constant k observed for pH 2.5 was 0.0573 min^{-1} with R^2 of 99.39%.

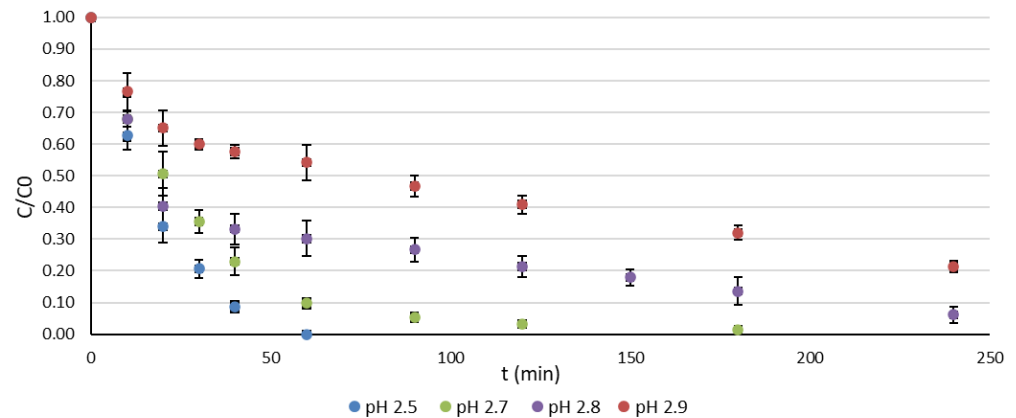


Figure 8. Duplicates of solution of $C_0 = 15 \text{ mg/L Cr(VI)}$, 5 mM citric acid and 1.2 g catalyst/L , in dark conditions and different pH values.

In order to clarify if the observed behavior was clearly tied to the pH factor, the experiments were reproduced using 3 mM HCl (pH 2.5) instead of citric acid. The results (Figure 9) indicate that low pH values partly assist in the reduction phenomenon and that inhibition still occurs due to Cr(III) precipitates, meaning that the presence of citric acid is important because not only lowers the pH, but also increases the solubility of Cr(III) species in these pH values [23], preventing active site occupation on the catalyst surface. This can also explain the inhibition when solar irradiation is provided in the system: As organic acids act as sacrificial agents in photocatalysis, the availability of citric acid decreases, leading to precipitate formed on the catalyst surface.

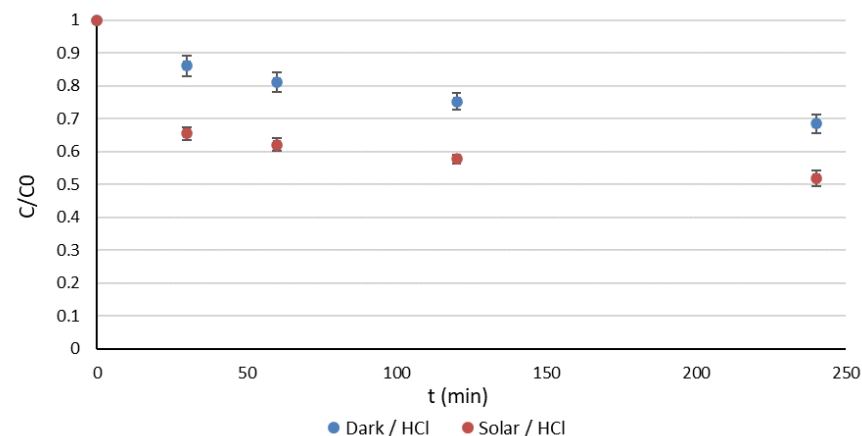


Figure 9. Duplicates of $C_0 = 15 \text{ mg/L Cr(VI)}$, in presence of 3 mM HCl and 1.2 g catalyst/L , under simulated solar irradiation and dark conditions, at pH 2.5.

This hypothesis was validated by increasing the citric acid concentration 5 times (25 mM , pH 2.4) in the hexavalent chromium solution. The results using 1.2 g/L of prepared SiNWAg/Cu catalyst under simulated solar irradiation and dark conditions are presented in Figure 10. Inhibition phenomena did not occur, and the reduction rate was increased drastically, especially in the case of photocatalysis, where the hexavalent chromium concentration in the solution dropped below the quantification limits of the

method over 10 min of reaction, achieving >99% reduction. In this case, the reaction constant k was calculated at 0.1689 and 0.4427 min^{-1} with R^2 of 98.67 and 99.27 for dark and solar conditions, respectively.

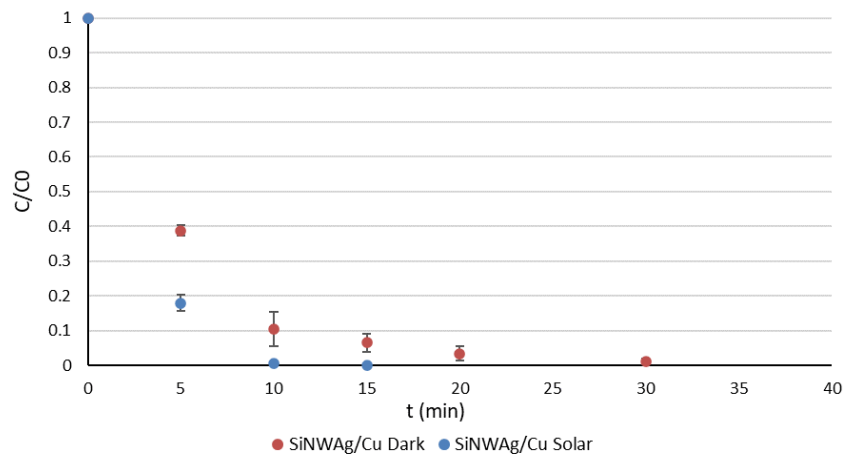


Figure 10. Triplicates of $C_0 = 15$ mg/L Cr(VI) reduction, in the presence of 25 mM citric acid and 1.2 g catalyst/L, under simulated solar irradiation and dark conditions, at pH 2.4.

The performance in higher hexavalent chromium and citric acid initial concentrations was also tested, and the results are depicted in Figure 11. When the initial Cr(VI) concentration was doubled to 30 mg/L, reduction was slower and required 150 min for its completion. By doubling the citric acid concentration, too (50 mM), 97% reduction was achieved in 60 min of irradiation. In the case of a high initial concentration of hexavalent chromium (120 mg/L), though, an inhibition of the reaction occurred once again after the first 20 min. Almost 40% of the initial 120 mg/L Cr(VI) was reduced during the first 20 min, leading to a fast and significant increase in the chromium species concentration that blocked the catalyst. This behavior is in accordance with the discussion above.

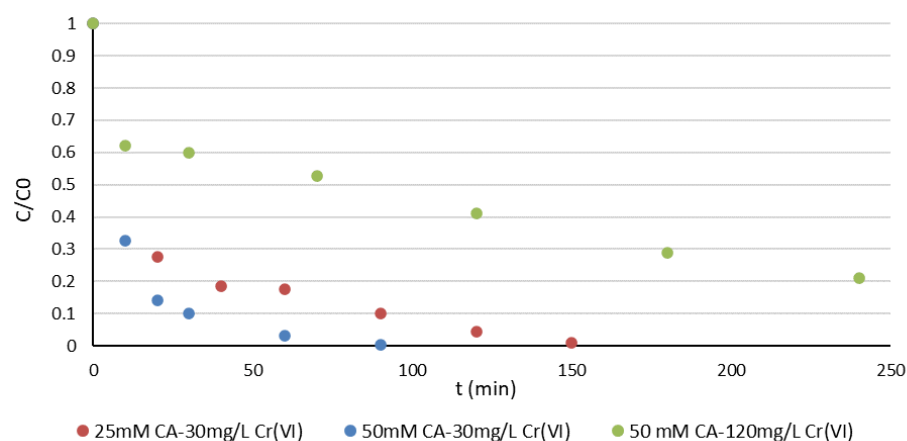
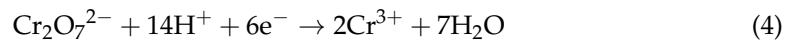
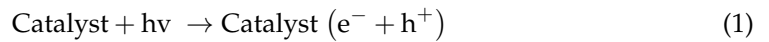


Figure 11. Cr(VI) C/C_0 ratio of different initial hexavalent chromium and citric acid (CA) concentrations, using 1.2 g catalyst/L, under simulated solar irradiation.

4. Discussion

The photocatalytic reduction mechanism of hexavalent chromium has been studied extensively, with a generally accepted pathway described in equations 1 to 5 [20,24–30]. The results presented indicate that the catalytic process is not purely photoinduced, contrary to previously reported findings [20]. In fact, in the conditions examined (5 mM citric acid), the irradiation of the solution seems to have an adverse effect to the reduction of hexavalent chromium. This behavior can be explained by the irreversible oxidation of the organic

acid that occurs due to the OH radicals developed by the electron/hole separation on the catalyst's surface under irradiation, as proposed by [24], which reduces the available concentration of citric acid for the reduction of the hexavalent chromium, as described in Equation (3), where $R = C_6H_8O_7$ in the case of citric acid being used as sacrificial agent.



As noted earlier (in Section 3.3), a sufficient reduction of hexavalent chromium can be obtained with the simultaneous presence of the organic acid and the Ag/Cu decorated SiNWs, without irradiation. This means that citric acid consumption as a sacrificial agent in the case of photocatalysis might be limiting the reduction phenomenon as its availability decreases. The exact nature and mechanism of the interaction among the metal decorated SiNWs, citric acid and hexavalent chromium is obscured even further by another phenomenon: As Cr(III) precipitate is formed, it deposits on the surface of the catalyst, occupying active sites [25] and thus inhibiting the reduction reaction both under dark and solar conditions. Citric acid is able to form soluble complexes with Cr(III) [23,26], though, preventing deposition on the catalyst's surface.

Summarizing the aforementioned, citric acid:

1. Lowers the pH increasing Cr(III) species solubility;
2. Forms a soluble complex with Cr(III), preventing active site occupation;
3. Acts as a sacrificial agent under irradiation.

In photocatalytic experiments, even though the citric acid acts as a hole scavenger to prevent the recombination of electron/hole pairs to increase the rate of the reduction, its own oxidation leads to faster deposition of Cr(III) on the catalyst surface and a slower reaction rate, since its concentration is reduced. This can be avoided by increasing the concentration of citric acid in the solution, as proved in Section 3.3, leading to a complete reduction of hexavalent chromium using the EoL Si prepared catalyst in 10 min of photocatalysis or 30 min in dark conditions (Figure 10). The optimum rates presented in this study are compared to previous reports in Table 1 below. It is obvious that, even without irradiation, in the conditions presented above, an efficient reduction rate is achieved.

Further experiments to clarify the exact role of citric acid as a function of the operating conditions are required in terms of studying the reaction mechanism. For the sake of future work, it should be mentioned that the use of a photocatalyst in powder form renders catalyst recovery difficult after the decontamination application. A method for stabilizing the recovered and modified silicon from EoL PVPs could increase the overall efficiency of the process even more.

Table 1. Photocatalytic reduction rates of hexavalent chromium in current and previous studies.

Catalyst	Catalyst Concentration (g/L)	Light Source	Volume (mL)	Cr(VI) C ₀ (mg/L)	k (min ⁻¹)	Reference
PV SiNWs/Ag/Cu	1.2	150 W Xe	600	15	0.4427	Current study
		Dark			0.1689	
TiO ₂	1	3 × 6 W Black Light	50	10	0.0049	27
TiO ₂ /Cu					0.0093	
CdS	1	300 W Xe	50	50	0.0245	28
ZnIn ₂ S ₄					0.0562	
ZIS/Cds-0.33	1	400 W metal halide	50	20	0.1790	29
ZnWO ₄					0.0085	
ZnWO ₄ /MB	1.67	400 W metal halide	30	20	0.0769	30
g-C ₃ N ₄ /DE					0.0016	
g-C ₃ N ₄ /DE/Ag/AgCl					0.0740	

5. Conclusions

Si was successfully recovered from end-of-life Si PVPs and cleaned. Afterwards, it was etched and doped with Ag/Cu through simple, electroless chemical methods for the preparation of a catalyst. The characterization of the material showed that the nature of the silicon recovered from EoL PVPs might affect the etching process and lead to reduced effectiveness of the catalyst.

The resulting material was tested in the heterogeneous catalysis of Cr(VI) reduction under simulated solar light irradiation and dark conditions in the presence of 5 mM of citric acid. Irradiation seems to inhibit the process, whereas, under dark conditions, 15 mg/L of hexavalent chromium are reduced $91 \pm 3\%$ in 240 min, in contrast with simulated solar irradiation, where a maximum of $81 \pm 4\%$ reduction is achieved after 240 min of irradiation. These results indicate that, contrary to what was previously reported, the observed reduction might not be attributable purely to photocatalytic activity. The series of experiments highlighted the importance of citric acid in the reduction reaction, due to its interaction with the produced Cr(III) species.

Nevertheless, the catalyst prepared from EoL PVP recovered silicon displayed promising results, achieving complete reduction of 15 mg/L of hexavalent chromium in 10 min of photocatalysis or 30 min under dark conditions using the EoL Si prepared catalyst and 25 mM of citric acid. These results indicate that the prepared catalyst could be reused for wastewater treatment applications such as the reduction of hexavalent chromium solution in the presence of citric acid.

Author Contributions: Methodology: C.P., K.P., P.T., P.K., E.R. and G.L.; investigation: G.L., E.R. and K.P.; writing—original draft preparation: C.P., K.P. and M.T.; writing—review and editing: G.L., E.R., P.T. and A.H.; supervision: K.P. and G.L. All authors have read and agreed to the published version of the manuscript.

Funding: This research has been co-financed by the European Union and Greek national funds through the Operational Program Competitiveness, Entrepreneurship and Innovation, under the call RESEARCH—CREATE—INNOVATE (project code: T1EDK-04249).

Institutional Review Board Statement: Not applicable.

Informed Consent Statement: Not applicable.

Data Availability Statement: Not applicable.

Conflicts of Interest: The authors declare no conflict of interest. The funders had no role in the design of the study; in the collection, analyses, or interpretation of data; in the writing of the manuscript or in the decision to publish the results.

References

1. IRENA; IEA-PVPS. *End-of-Life Management: Solar Photovoltaic Panels*; National Renewable Energy Lab.: Golden, CO, USA, 2016.
2. Masoumian, M.; Kopacek, P. End-of-Life Management of Photovoltaic Modules. *IFAC-Pap.* **2015**, *48*, 162–167. [[CrossRef](#)]
3. Savvilitidou, V.; Antoniou, A.; Gidakos, E. Toxicity assessment and feasible recycling process for amorphous silicon and CIS waste photovoltaic panels. *Waste Manag.* **2017**, *59*, 394–402. [[CrossRef](#)] [[PubMed](#)]
4. Sica, D.; Malandrino, O.; Supino, S.; Testa, M.; Lucchetti, M.C. Management of end-of-life photovoltaic panels as a step towards a circular economy. *Renew. Sustain. Energy Rev.* **2018**, *82*, 2934–2945. [[CrossRef](#)]
5. Buitrago, E.; Novello, A.M.; Meyer, T. Third-Generation Solar Cells: Toxicity and Risk of Exposure. *HCA* **2020**, *103*, e2000074. [[CrossRef](#)]
6. Doi, T.; Tsuda, I.; Unagida, H.; Murata, A.; Sakuta, K.; Kurokawa, K. Experimental study on PV module recycling with organic solvent method. *Sol. Energy Mater. Sol. Cells* **2001**, *67*, 397–403. [[CrossRef](#)]
7. Granata, G.; Pagnanelli, F.; Moscardini, E.; Havlik, T.; Toro, L. Recycling of photovoltaic panels by physical operations. *Sol. Energy Mater. Sol. Cells* **2014**, *123*, 239–248. [[CrossRef](#)]
8. Theocharis, M.; Pavlopoulos, C.; Kousi, P.; Hatzikioseyan, A.; Zarkadas, I.; Tsakiridis, P.E.; Remoundaki, E.; Zoumboulakis, L.; Lyberatos, G. An Integrated Thermal and Hydrometallurgical Process for the Recovery of Silicon and Silver From End-of-life Crystalline Si Photovoltaic Panels. *Waste Biomass-Valorization* **2022**, *13*, 4027–4041. [[CrossRef](#)]
9. Theocharis, M.; Tsakiridis, P.E.; Kousi, P.; Hatzikioseyan, A.; Zarkadas, I.; Remoundaki, E.; Lyberatos, G. Hydrometallurgical Treatment for the Extraction and Separation of Indium and Gallium from End-of-Life CIGS Photovoltaic Panels. *Mater. Proc.* **2021**, *5*, 51. [[CrossRef](#)]
10. Corcelli, F.; Ripa, M.; Ulgiati, S. End-of-life treatment of crystalline silicon photovoltaic panels. An energy-based case study. *J. Clean. Prod.* **2017**, *161*, 1129–1142. [[CrossRef](#)]
11. Duflou, J.R.; Peeters, J.R.; Altamirano, D.; Bracquene, E.; Dewulf, W. Demanufacturing photovoltaic panels: Comparison of end-of-life treatment strategies for improved resource recovery. *CIRP Ann.* **2018**, *67*, 29–32. [[CrossRef](#)]
12. Pavlopoulos, C.; Kelesi, M.; Michopoulos, D.; Papadopoulou, K.; Lymperopoulou, T.; Skaropoulou, A.; Tsvivilis, S.; Lyberatos, G. Management of end-of-life photovoltaic panels based on stabilization using Portland cement. *Sustain. Chem. Pharm.* **2022**, *27*, 100687. [[CrossRef](#)]
13. Liu, D.; Ma, J.; Long, R.; Gao, C.; Xiong, Y. Silicon nanostructures for solar-driven catalytic applications. *Nano Today* **2017**, *17*, 96–116. [[CrossRef](#)]
14. Srivastava, S.; Kumar, D.; Schmitt, S.W.; Sood, K.; Christiansen, S.; Singh, P. Large area fabrication of vertical silicon nanowire arrays by silver-assisted single-step chemical etching and their formation kinetics. *Nanotechnology* **2014**, *25*, 175601. [[CrossRef](#)] [[PubMed](#)]
15. Chiou, A.H.; Chien, T.; Su, C.K.; Lin, J.F.; Hsu, C.Y. The effect of differently sized Ag catalysts on the fabrication of a silicon nanowire array using Ag-assisted electroless etching. *Curr. Appl. Phys.* **2013**, *13*, 717–724. [[CrossRef](#)]
16. Salhi, B.; Hossain, M.K.; Al-Sulaiman, F. Wet-chemically etched silicon nanowire: Effect of etching parameters on the morphology and optical characterizations. *Sol. Energy* **2018**, *161*, 180–186. [[CrossRef](#)]
17. Naama, S.; Hadjersi, T.; Menari, H.; Nezzal, G.; Ahmed, L.B.; Lamrani, S. Enhancement of the tartrazine photodegradation by modification of silicon nanowires with metal nanoparticles. *Mater. Res. Bull.* **2016**, *76*, 317–326. [[CrossRef](#)]
18. Nguyen, T.H.; Vuong, V.C.; Nguyen, D.L. Mechanism of the photocatalytic activity of p-Si(100)/n-ZnO nanorods heterojunction. *Mater. Chem. Phys.* **2018**, *204*, 397–402. [[CrossRef](#)]
19. Brahiti, N.; Hadjersi, T.; Amirouche, S.; Menari, H.; El Kechai, O. Photocatalytic degradation of cationic and anionic dyes in water using hydrogen-terminated silicon nanowires as catalyst. *Int. J. Hydrogen Energy* **2018**, *43*, 11411–11421. [[CrossRef](#)]
20. Fellahi, O.; Barras, A.; Pan, G.; Coffinier, Y.; Hadjersi, T.; Maamache, M.; Szunerits, S.; Boukherroub, R. Reduction of Cr(VI) to Cr(III) using silicon nanowire arrays under visible light irradiation. *J. Hazard. Mater.* **2016**, *304*, 441–447. [[CrossRef](#)]
21. Xia, S.; Jeyakumar, P.; Rinklebe, J.; Ok, Y.S.; Bolan, N.; Wang, H. A critical review on bioremediation technologies for Cr(VI)-contaminated soils and wastewater. *Crit. Rev. Environ. Sci. Technol.* **2019**, *49*, 1027–1078. [[CrossRef](#)]
22. Wu, S.L.; Zhang, T.; Zheng, R.T.; Cheng, G.A. Facile morphological control of single-crystalline silicon nanowires. *Appl. Surf. Sci.* **2012**, *258*, 9792–9799. [[CrossRef](#)]
23. Remoundaki, E.; Hatzikioseyan, A.; Tsezos, M. A systematic study of chromium solubility in the presence of organic matter: Consequences for the treatment of chromium-containing wastewater. *J. Chem. Technol. Biotechnol.* **2007**, *82*, 802–808. [[CrossRef](#)]
24. Hongbo, H.; Zhuangzhu, L.; Changlin, Y. Water-soluble natural organic acid for highly efficient photoreduction of hexavalent chromium. *J. Chem. Sci.* **2020**, *132*, 113. [[CrossRef](#)]
25. Ngo, A.; Nguyen, H.; Hollmann, D. Critical Assessment of the Photocatalytic Reduction of Cr(VI) over Au/TiO₂. *Catalysts* **2018**, *8*, 606. [[CrossRef](#)]
26. Montesinos, V.; Salou, C.; Meichtry, J.; Colbeau-Justin, C.; Litter, M. Role of Cr(III) deposition during the photocatalytic transformation of hexavalent chromium and citric acid over commercial TiO₂ samples. *Photochem. Photobiol. Sci.* **2016**, *15*, 228–234. [[CrossRef](#)] [[PubMed](#)]
27. Ran, Y.; Li, L.; Yingying, X.; Yuening, Y.; Alok, D.B.; Chii, S. Enhanced photocatalytic reduction of chromium (VI) by Cu-doped TiO₂ under UV-A irradiation. *Sep. Purif. Technol.* **2018**, *190*, 53–59. [[CrossRef](#)]

28. Guping, Z.; Dongyun, C.; Najun, L.; Qingfeng, X.; Hua, L.; Jinghui, H.; Jianmei, L. Preparation of ZnIn₂S₄ nanosheet-coated CdS nanorod heterostructures for efficient photocatalytic reduction of Cr(VI). *Appl. Catal. B Environ.* **2018**, *232*, 164–174. [[CrossRef](#)]
29. Hongbo, H.; Zhuangzhu, L.; Zhen-Yu, T.; Changlin, Y. Controllable construction of ZnWO₄ nanostructure with enhanced performance for photosensitized Cr(VI) reduction. *Appl. Surf. Sci.* **2019**, *490*, 460–468. [[CrossRef](#)]
30. Hongbo, H.; Jiade, L.; Changlin, Y.; Zhuangzhu, L. Surface decoration of microdisk-like g-C₃N₄/diatomite with Ag/AgCl nanoparticles for application in Cr(VI) reduction. *Sustain. Mater. Technol.* **2019**, *22*, e00127. [[CrossRef](#)]

Disclaimer/Publisher's Note: The statements, opinions and data contained in all publications are solely those of the individual author(s) and contributor(s) and not of MDPI and/or the editor(s). MDPI and/or the editor(s) disclaim responsibility for any injury to people or property resulting from any ideas, methods, instructions or products referred to in the content.